

LINEAR KINETIC EFFECTS OF CORE PLASMA ON LOW FREQUENCY ALFVÉN AND ACOUSTIC EIGENMODES IN TOKAMAKS

I. CHAVDAROVSKI

Korea Institute of Fusion Energy, Daejeon, Republic of Korea

Email: chavdarovski@gmail.com

F. ZONCA

C.R. ENEA Frascati, Rome, Italy

L. CHEN

Dept. of Physics and Astronomy, Univ. of California, Irvine CA, U.S.A.

Institute for Fusion Theory and Simulation, Zhejiang University, Hangzhou, PR China

Abstract

The resonant and non-resonant effects of core plasma on the excitation of low frequency modes with $\omega < \omega_{BAE}$, such as Beta-induced Alfvén Acoustic Eigenmodes (BAAEs) and Kinetic Ballooning Modes (KBMs) are examined in the framework of the generalized fishbone-like dispersion relation. The formalism of the fishbone-like equation contains all the necessary ingredients to describe the features of these low frequency fluctuations, and explain experimental findings. Core plasma properties (diamagnetic frequency and precession resonance with trapped ions) strongly affect the excitation of the modes, and in the case of BAAEs more effectively than the energetic particles. The diamagnetic frequency of the core plasma also contributes to the coupling of the BAAEs with the KBMs, thus affecting the excitation and polarization of both modes. Energetic particles can still provide a non-resonant drive to some of the low frequency modes.

1. INTRODUCTION

Electromagnetic modes with frequencies of the order of thermal ions periodic motion $\omega_{Ti} = (T_i/m_i)^{1/2}/(qR_0)$ and $\omega_{Bi} \sim \epsilon^{1/2}\omega_{Ti}$ and precessional motion of trapped particles $\bar{\omega}_{Di}$, as well as their diamagnetic frequency $\omega_{*pi} = (T_i c/e_s B)(\mathbf{k} \times \mathbf{b}) \cdot \nabla(T_i)/n_i$, have been observed on several machines, such as DIII-D and HL-2A tokamaks. One of these modes named Beta-induced Alfvén acoustic eigenmode (BAAE) has been theoretically described by MHD theory [1] and shown to have a mixed Alfvénic and acoustic polarization and frequency $\omega_{BAAE} \sim (T_e/T_i)^{1/2}\omega_{Ti}$. Several experiments have reported resonant energetic particle (EP) excitation of low frequency BAAEs, and wrongly identified them as a cause of EP losses, on a basis of their frequency range. However, theoretical analysis shows that energetic particles are not efficient in resonantly driving the BAAEs [2]. Moreover, the BAAEs are heavily damped by thermal ions and parallel electric field [3, 4], and not easy to excite. These modes are however coupled with the Kinetic Ballooning Mode (KBM) branch of low frequency Alfvénic oscillations [5] with frequency close to ω_{*pi} , but significantly smaller damping rate. Diamagnetic effects of core plasma contribute to the coupling of the BAAEs and KBMs, thus affecting the excitation and polarization of both modes, and in the case of BAAEs significantly reducing the damping rate [4]. Precession resonance with trapped ions which occurs in this frequency range, is expected to have a more important role for the excitation of the low frequency modes than energetic particles.

Additionally, non-resonant effects of the background (or hot) plasma might provide enough drive to destabilize low frequency modes, in which case the mode frequency is not determined by particle resonance, but by the thermal plasma diamagnetic frequency ω_{*pi} [6]. The modes previously recognized as BAAEs in experiments are much more likely to be excited in this way, and hence should be identified as reactive modes. A significant number of experiments on DIII-D tokamak [6] have shown this type of modes appearing in a "Christmas lights" pattern due to the time evolution of the q -profile which passes through several rational numbers $q = m/n$, with m and n being the poloidal and toroidal numbers, respectively. Common feature of these modes, labeled Low Frequency Modes (LFMs) is that they appear near q_{min} of a reversed shear profile, and they are driven by high electron temperature T_e , but modest β_i . Their polarization is Alfvénic and the instability is reactive in nature.

The closeness of the modes to the ion resonant frequencies has prompted a development of a kinetic treatment [3] of both circulating [7] and trapped particles [8, 4] to properly describe these low frequency specimen. Due to the large number of activities in this frequency range the identification of the mode has to include the frequency, damping rate and its polarization. The latter is however difficult to determine experimentally, which is one of the reasons why analytical tools such as the Generalized fishbone-like dispersion relation (GFLDR) is useful for systematic study of these low frequency modes. In this framework the dispersion relation of the mode is given by [5]

$$i\Lambda(\omega) = \delta\bar{W}_f + \delta\bar{W}_k, \quad (1)$$

which is a unifying picture for various Alfvénic fluctuations, as well as Energetic particle continuum modes (EPMs). Here, Λ is the general inertia and represents the physics inside the inertial layer, while $\delta\bar{W}_f$ and $\delta\bar{W}_k$ are the ideal region background MHD and energetic particle kinetic contribution, respectively. The scope of this work is to show that the GFLDR in its most general form contains all the ingredients necessary to describe the behavior of the low frequency modes and their mutual interaction.

2. THEORETICAL MODEL

We adopt the ballooning formalism in the space of the extended poloidal angle θ , for low $\beta = O(\epsilon^2)$ axisymmetric (s, α) plasma equilibrium, with $s = rq'/q$ being the finite magnetic shear and $\alpha = -R_0q^2\beta'$ the ballooning drive. We describe the plasma with three fluctuating scalar fields: $\delta\phi$, $\delta\psi$ and δB_{\parallel} . Eq. (1) is obtained by asymptotic matching of the "singular" inertial layer and "regular" ideal region solutions of the eigenmode (vorticity) equation for $\delta\psi$ at the modes rational surface [5]. In the inertial layer the fields vary on a short scale $\theta_0 \sim O(1)$ and on a long scale $\theta_1 \sim (\beta^{1/2})$, while their governing equations in the long wavelength limit are the vorticity equation [5, 7]

$$B\mathbf{b} \cdot \nabla \left[\frac{1}{B} \frac{k_{\perp}^2}{k_{\parallel}^2} \mathbf{b} \cdot \nabla \delta\psi \right] + \frac{\omega^2}{v_A^2} \left(1 - \frac{\omega_{*pi}}{\omega} \right) \frac{k_{\perp}^2}{k_{\parallel}^2} \delta\phi + \frac{\alpha}{q^2 R^2} g(\theta) \delta\psi = \left\langle \frac{4\pi e}{k_{\parallel}^2 c^2} \omega \omega_{di} \delta K_i \right\rangle, \quad (2)$$

and quasi-neutrality condition

$$\left(1 + \frac{1}{\tau} \right) (\delta\phi - \delta\psi) = \frac{T_i}{ne} \langle \delta K_i - \delta K_e \rangle. \quad (3)$$

Here δK_i and δK_e represent the compressional parts of the perturbed particle distribution function δf_s , for $s = i, e$, while $\langle (\dots) \rangle = \int d\mathbf{v}(\dots)$ denotes integration in velocity space.

The perpendicular k_\perp and poloidal k_θ wave numbers satisfy $k_\perp^2/k_\theta^2 = 1 + (s\theta - \alpha \sin \theta)^2$, while $g(\theta) = \cos \theta + [s\theta - \alpha \sin \theta] \sin \theta$, $\tau = T_e/T_i$ and $n_e = n_i = n$. Further, we will use the more convenient variables $\delta\Phi = (k_\perp/k_\theta) \delta\phi$ and $\delta\Psi = (k_\perp/k_\theta) \delta\psi$, which represented in series of powers of $\beta^{1/2}$ give (see [7] and [8]) $\delta\Psi^{(0)} = \delta\Psi^{(0)}(\theta_1)$, $\delta\Psi^{(1)} = 0$ and $\delta\Phi^{(1)} \simeq \delta\Phi^{(0)} + \delta\Phi_s(\theta_1) \sin \theta_0$. Here, $\delta\Phi_s(\theta_1) \sin \theta_0$ is the sinusoidal a.c. term of the perturbed electric potential, while $\delta\Phi_c(\theta_1) \cos \theta_0$ was dropped, since $\delta\Phi_c \ll \delta\Phi_s$ [7, 8].

For trapped ions the distribution function is written as [8]

$$\begin{aligned} \delta K_i = & - Q f_{0i} \left(\frac{e}{m} \right)_i \frac{1}{\omega - \bar{\omega}_{di}} \frac{k_\theta}{k_\perp} \left[\frac{\bar{\omega}_{di}}{\omega} \delta\Psi^{(0)} + \delta\Phi^{(0)} - \delta\Psi^{(0)} \right] \\ & - Q f_{0i} \left(\frac{e}{m} \right)_i \frac{1}{(\omega - \bar{\omega}_{di})^2 - \omega_b^2} \frac{k_\theta}{k_\perp} \left[\bar{\omega}_{di} \delta\Phi^{(0)} \xi + (\omega - \bar{\omega}_{di}) \delta\Phi_s \right] \sin \theta . \end{aligned} \quad (4)$$

The second term contains the $\bar{\omega}_d \pm \omega_b$ resonances and is an essential contribution to the inertial layer dynamics, while the first one containing $\bar{\omega}_{di}$ resonance is found to be of order $\xi = k_\perp/k_\theta$ smaller than the second one. The ratio k_\perp/k_θ is large in the inertial layer, but of $O(1)$ in the ideal region, hence the precession resonance will not contribute to the inertial layer dynamics, aside from the quasineutrality condition. In the ideal region, however we can expect the thermal ion precession resonance to appear on the right hand side of Eq.(1), and have effect on modes of the order of $\bar{\omega}_{di}$, i.e. low frequency modes.

The quasineutrality condition in zeroth order gives [4] $\delta\Phi^{(0)} = I_\Phi(\omega, \omega_{Di,e}, \omega_{*i,e}) \delta\Psi^{(0)}$, where $I_\Phi(\omega, \omega_{Di,e}, \omega_{*i,e})$ represents a deviation from the ideal MHD limit $\delta E_\parallel = 0$, obtained for $I_\Phi = 1$. For most of the spectrum of the Alfvénic fluctuations, except frequencies near $\bar{\omega}_{D,ei}$, we have $I_\Phi \simeq 1$ thus recovering the ideal MHD condition. Around the specific precession frequencies of the ions and electrons, $I_\Phi \neq 1$ which gives a finite parallel electric field as a result of the slow precessional motion of the electrons and ions in opposite directions. This electric field might have important implications on the collisionless micro-tearing effects, but also contribute to the loss of particles on the trapped/passing border.

Next order ($\beta^{1/2}$) quasineutrality condition gives $\delta\Phi_s(\theta_1) = S(\omega, \omega_{Bi}, \bar{\omega}_{Di}, \omega_{Ti}) \xi \delta\Phi^{(0)}$, which recalling $\delta\Psi^{(1)} = 0$ makes the function $|S|$ a measure of how much the polarization deviates from pure Alfvénic due to the parallel a.c. electric field. The polarization term S was calculated from the quasineutrality condition [8] to obtain:

$$S = - \frac{N_1(\frac{\omega}{\omega_{Ti}}) + \Delta N_1(\frac{\omega}{\omega_{Ti}}) + \sqrt{2\epsilon} P_2(\frac{\omega}{\bar{\omega}_{Di}}, \frac{\omega_{Bi}}{\bar{\omega}_{Di}})}{1 + \frac{1}{\tau} + D_1(\frac{\omega}{\omega_{Ti}}) + \Delta D_1(\frac{\omega}{\omega_{Ti}}) + \sqrt{2\epsilon} \left[P_1(\frac{\omega}{\bar{\omega}_{Di}}, \frac{\omega_{Bi}}{\bar{\omega}_{Di}}) - P_2(\frac{\omega}{\bar{\omega}_{Di}}, \frac{\omega_{Bi}}{\bar{\omega}_{Di}}) \right]}, \quad (5)$$

where $P_1(\omega/\bar{\omega}_{Di}, \omega_{Bi}/\bar{\omega}_{Di})$ and $P_2(\omega/\bar{\omega}_{Di}, \omega_{Bi}/\bar{\omega}_{Di})$ come from the trapped particles dynamics:

$$\begin{aligned} P_1(\omega/\bar{\omega}_{Di}, \omega_{Bi}/\bar{\omega}_{Di}) &= -2 \frac{\omega^2}{\bar{\omega}_{Di}^2} \left[\left(1 - \frac{\omega_{*n}}{\omega} + \frac{3}{2} \frac{\omega_{*T}}{\omega}\right) G_2 - \frac{\omega_{*T}}{\omega} G_4 \right], \\ P_2(\omega/\bar{\omega}_{Di}, \omega_{Bi}/\bar{\omega}_{Di}) &= -2 \frac{\omega}{\bar{\omega}_{Di}} \left[\left(1 - \frac{\omega_{*n}}{\omega} + \frac{3}{2} \frac{\omega_{*T}}{\omega}\right) G_4 - \frac{\omega_{*T}}{\omega} G_6 \right], \end{aligned}$$

and we have denoted

$$G_n = \frac{1}{\pi^{1/2}} \int_{-\infty}^{\infty} \frac{e^{-x^2} x^n}{(\omega/\bar{\omega}_{Di} - x^2)^2 - (\omega_{Bi}/\bar{\omega}_{Di})^2 x^2} dx,$$

for $n = 2, 4, 6, 8$. The G_n integrals yield [8]

$$\begin{aligned}
 G_2 &= \frac{\bar{\omega}_{Di}/\omega_{Bi}}{\Omega_1 + \Omega_2} [\Omega_1 Z(\Omega_1) - \Omega_2 Z(\Omega_2)] \quad , \quad (6) \\
 G_4 &= \frac{\bar{\omega}_{Di}/\omega_{Bi}}{\Omega_1 + \Omega_2} [\Omega_1^2 - \Omega_2^2 + \Omega_1^3 Z(\Omega_1) - \Omega_2^3 Z(\Omega_2)] \quad , \\
 G_6 &= \frac{\bar{\omega}_{Di}/\omega_{Bi}}{\Omega_1 + \Omega_2} [(1/2)(\Omega_1^2 - \Omega_2^2) + \Omega_1^4 - \Omega_2^4 + \Omega_1^5 Z(\Omega_1) - \Omega_2^5 Z(\Omega_2)] \quad , \\
 G_8 &= \frac{\bar{\omega}_{Di}/\omega_{Bi}}{\Omega_1 + \Omega_2} [(3/4)(\Omega_1^2 - \Omega_2^2) + (1/2)(\Omega_1^4 - \Omega_2^4) + \Omega_1^6 - \Omega_2^6 + \Omega_1^7 Z(\Omega_1) - \Omega_2^7 Z(\Omega_2)] \quad ,
 \end{aligned}$$

where $Z(x) = 1/\sqrt{\pi} \int_{-\infty}^{\infty} e^{-y^2}/(y-x) dy$ is the plasma dispersion function that contains the $\omega = \bar{\omega}_{Di} \pm \omega_{Bi}$ resonances in the parameters Ω_1 and Ω_2 given by

$$\Omega_1 = \frac{\frac{\omega_{Bi}}{\bar{\omega}_{Di}} + \sqrt{\left(\frac{\omega_{Bi}}{\bar{\omega}_{Di}}\right)^2 + 4\frac{\omega}{\bar{\omega}_{Di}}}}{2} \quad \text{and} \quad \Omega_2 = \frac{-\frac{\omega_{Bi}}{\bar{\omega}_{Di}} + \sqrt{\left(\frac{\omega_{Bi}}{\bar{\omega}_{Di}}\right)^2 + 4\frac{\omega}{\bar{\omega}_{Di}}}}{2} .$$

In Eq. (5), the functions

$$D_1(x) = x \left(1 - \frac{\omega_{*ni}}{\omega}\right) Z(x) - \frac{\omega_{*Ti}}{\omega} x [x + (x^2 - 1/2)Z(x)] \quad (7)$$

and $N_1(x) = 2(\bar{\omega}_{Di}/\omega_{Ti})N(x)$, with

$$N(x) = \left(1 - \frac{\omega_{*ni}}{\omega}\right) [x + (1/2 + x^2)Z(x)] - \frac{\omega_{*Ti}}{\omega} [x(1/2 + x^2) + (1/4 + x^4)Z(x)] \quad , \quad (8)$$

come from the well circulating particles dynamics [7]. These functions contain the $\omega = \omega_{Ti}$ resonance and are strictly valid for well circulating particles. In order to extend their validity virtually to $\omega \simeq 0$, correction functions

$$\Delta D_1(x) = \frac{x}{\pi^{1/2}} \int_0^{\infty} e^{-y} \ln \left(\frac{x + \sqrt{2\epsilon y}}{x - \sqrt{2\epsilon y}} \right) \left[1 - \frac{\omega_{*ni}}{\omega} - \frac{\omega_{*Ti}}{\omega} \left(y - \frac{3}{2} \right) \right] dy \quad (9)$$

and

$$\Delta N_1(x) = \frac{\bar{\omega}_{Di}/\omega_{Ti}}{\pi^{1/2}} \int_0^{\infty} y e^{-y} \ln \left(\frac{x + \sqrt{2\epsilon y}}{x - \sqrt{2\epsilon y}} \right) \left[1 - \frac{\omega_{*ni}}{\omega} - \frac{\omega_{*Ti}}{\omega} \left(y - \frac{3}{2} \right) \right] dy \quad , \quad (10)$$

were added [8]. The corrections also account for the finite trapped particle fraction and reduce the circulating population by $\sqrt{2\epsilon}$. This model is a mixture of deeply trapped and well circulating particles, so some error is always expected when working in the low frequency regime. However, it has been shown that this reduced model recovers well the low and high frequency behavior of hot plasmas [8], and even gives new insights which are consistent with the experiments.

The vorticity equation expanded to the second order in the inertial layer reduces to the form $(\partial^2/\partial\theta_1^2)\delta\Psi^{(0)} + \Lambda^2\delta\Psi^{(0)} = 0$, where the general expression of Λ^2 can be written as [8]

$$\Lambda^2/I_{\Phi} = \frac{\omega^2}{\omega_A^2} \left(1 - \frac{\omega_{*pi}}{\omega}\right) + \Lambda_{cir}^2 + \Lambda_{tra}^2 \quad , \quad (11)$$

with Λ_{cir}^2 [7] and Λ_{tra}^2 [8] being the circulating and trapped particle contributions, respectively. Here

$$\Lambda_{tra}^2 = \frac{\omega^2 \omega_{Bi}^2}{\omega_A^2 \bar{\omega}_{Di}^2} \frac{q^2}{\sqrt{2\epsilon}} [P_3 + (P_2 - P_3)S(\omega, \bar{\omega}_{Di}, \omega_{Bi}, \omega_{Ti})] \quad (12)$$

and

$$P_3 = -2 \left[\left(1 - \frac{\omega_{*n}}{\omega} + \frac{3}{2} \frac{\omega_{*T}}{\omega}\right) G_6 - \frac{\omega_{*T}}{\omega} G_8 \right].$$

The circulating particle term in Eq. (11) contains the well circulating response [7] and the previously mentioned corrections

$$\Lambda_{cir}^2 = q^2 \frac{\omega \omega_{Ti}}{\omega_A^2} \left[\left(1 - \frac{\omega_{*ni}}{\omega}\right) \left(F\left(\frac{\omega}{\omega_{Ti}}\right) + \Delta F\left(\frac{\omega}{\omega_{Ti}}\right) \right) - \frac{\omega_{*Ti}}{\omega} \left(G\left(\frac{\omega}{\omega_{Ti}}\right) + \Delta G\left(\frac{\omega}{\omega_{Ti}}\right) \right) + \frac{\omega \omega_{Ti}}{4 \bar{\omega}_{Di}^2} \left(N_1\left(\frac{\omega}{\omega_{Ti}}\right) + \Delta N_1\left(\frac{\omega}{\omega_{Ti}}\right) \right) S(\omega, \bar{\omega}_{Di}, \omega_{Bi}, \omega_{Ti}) \right],$$

which, in the $\epsilon \rightarrow 0$ limit reduces to the well circulating particle equations of Ref. [7] with:

$$\begin{aligned} F(x) &= x(x^2 + 3/2) + (x^4 + x^2 + 1/2) Z(x), \\ G(x) &= x(x^4 + x^2 + 2) + (x^6 + x^4/2 + x^2 + 3/4) Z(x). \end{aligned} \quad (13)$$

The corrections are given by [8]:

$$\Delta F(x) = \frac{1}{\pi^{1/2}} \int_0^\infty e^{-y} \ln \left(\frac{x + \sqrt{2\epsilon y}}{x - \sqrt{2\epsilon y}} \right) \frac{y^2}{4} dy, \quad (14)$$

and

$$\Delta G(x) = \frac{1}{\pi^{1/2}} \int_0^\infty e^{-y} \ln \left(\frac{x + \sqrt{2\epsilon y}}{x - \sqrt{2\epsilon y}} \right) \frac{y^2}{4} \left(y - \frac{3}{2} \right) dy. \quad (15)$$

The fluid limit ($\omega \gg \omega_{ti}$ and $\omega_* \rightarrow 0$) of Eq. (11) is $\Lambda^2 = [\omega^2 - \omega_{BAE}^2(1 + \delta(\tau, q, \omega))]/\omega_A^2$, which contains the known BAE accumulation point $\omega_{BAE}^2 = 2T_i(7/4 + \tau)/(m_i R_0^2)$, with a higher order correction $\delta(\tau, q, \omega)$ [9]. The Beta-induced Alfvén eigenmode is located in the gap below the continuum and its frequency is a function of ω_{*pi} [7, 4]. At low frequency the same equation gives the Rosenbluth-Hinton inertia enhancement [10, 11]

$$\Lambda^2 = \frac{\omega^2}{\omega_A^2} \left(1 - \frac{\omega_{*pi}}{\omega}\right) (1 + 1.6q^2\epsilon^{-1/2} + 0.5q^2), \quad (16)$$

which contains the known ion polarization term, in addition to the ion compression in toroidal geometry, i.e. neoclassical enhancement. The term I_ϕ in Eq. (11) acts as an additional inertia enhancement due to the slow precessional motion of ions and electrons around the torus in opposite directions.

Several different derivations of $\delta\bar{W}_f$ are known, one of which shown here [12]

$$\delta\bar{W}_f \simeq \frac{\pi}{|s|} \left[\frac{s^2}{4} - \frac{3\alpha|s|}{2} + \frac{5\alpha^2 s^2}{32} + \frac{45\alpha^4}{128} - \left(1 + \frac{\alpha}{2}\right) e^{-\frac{1}{|s|}} \right], \quad (17)$$

is valid for $|s| \sim \alpha^2$ and small $\alpha = (1 + \tau)(1 + \eta_i)q^2\beta_i/\epsilon_{ni} + q^2\beta_E/\epsilon_{nE}$, where $\epsilon_{ns} = L_{ns}/R_0$ for $s = i, E$, and L_{ns} are the density gradient scales of the thermal and energetic ions. The $\delta\bar{W}_f$

term accounts for the thermal electron temperature in τ and non-resonant EP effects (β_E), as well as the sharp spacial gradient of EPs through L_{nE} . Detailed discussion about the $\delta\bar{W}_k$ term can be found in Ref. [13]. Here, due to the low frequency we focus on the resonant interaction of the modes with the particle precessional motion, neglecting the bounce frequency resonance. A fairly exhaustive analysis of the modes can be conducted by using the EP $\delta\bar{W}_k$ term of Ref. [13] for trapped ions

$$\delta\bar{W}_{kt} = \frac{2\pi^2}{|s|} \frac{e^2}{mc^2} qR_0B_0 \int d\varepsilon \int d\mu \left(\frac{\bar{\omega}_D}{k_\theta} \right)^2 \left(1 - \frac{\Delta_{b0}}{(1 + \Delta_{b0}^2)^{1/2}} \right) \frac{\tau_b QF_0}{\bar{\omega}_D - \omega}, \quad (18)$$

where $Qf_0 = (\omega\partial_\varepsilon + \hat{w}_*)_s f_0$, $\tau_b = 2\pi/\omega_b$, while $\Delta_{b0}^2 = k_\theta^2(\rho_L^2 + \rho_b^2)/2$ accounts for both finite Larmor radius (ρ_L) and finite banana orbit width (ρ_b). This term was originally derived for energetic particles [5], but it also applies to thermal ions and electrons in the small FLR/FOW limit ($\rho_L, \rho_b \rightarrow 0$). While for energetic particles the spacial gradient term \hat{w}_* is dominant, for thermal particles the energy derivative is of the same order. Here, we remind the reader that for thermal electrons the frequencies in $\delta\bar{W}_{kt}$ should be replaced with $\omega_{*i} \rightarrow -\tau\omega_{*i}$, $\bar{\omega}_{Di} \rightarrow -\tau\bar{\omega}_{Di}$ and $\omega_{bi} \rightarrow \sqrt{\tau}\omega_{bi}$, giving another dependence of the modes on the electron temperature. Since ω_{*p} and $\bar{\omega}_D$ for electrons and ions are of the same order, both $\delta\bar{W}_{kt}$ terms should be kept in the analysis on the righthand side as $\delta\bar{W}_{ki} + \delta\bar{W}_{ke}$. However, due to the opposite signs of the resonant frequencies they would likely affect different modes, at different times. Eq. (18) for thermal particles has strong effects in low frequency regimes ($\omega \sim \omega_{*p}, \bar{\omega}_D$), but not around ω_{BAE} .

3. DISPERSION RELATION OF THE LOW FREQUENCY MODES

The GFLDR contains all the elements of the kinetic thermal ion gap necessary to identify and study low frequency modes and their polarization, including the background plasma MHD potential, resonant and non-resonant energetic particle drive, as well as thermal ion and electron dynamics. Hence, the equation as roots has both the reactive low frequency instability [6], as well as several different modes in this frequency range like BAEs, EPs, KBMs, BAAEs and MHD modes [14]. For modes located at the vanishing shear, i.e. q_{min} of a reversed shear profile, the LHS of Eq.(1) should be expanded around $s = 0$, as done in Ref.[13]. The equation $\Lambda = 0$ was solved in Ref. [4] and the accumulation points were obtained for the three modes shown in FIG. 1., without the presence of EPs. Since the functions in Λ are transcendental, additional roots in the negative complex plane appear, in which case for each branch only the most unstable mode is physically relevant. The roots numbered 1 – 3 are mixed Alfvén-acoustic, and they do not show excitation for the parameters considered in this work. For low η_i and Ω_* the KBMs is marginally stable and has a frequency close to ω_{*pi} , i.e, proportional to the n - mode number up to values of $\omega/\omega_{ti} \sim 1.5$. For increasing ω_{*pi} this behavior is modified due to the coupling with the BAAE [4] and BAE [7], and the KBM is becoming more damped. In FIG. 1. the KBM is shown for $\eta_i = 1$ and $\Omega_* = 0.8$ marked with an 'x' in the negative complex plane. The coupling to the KBM is of great importance for the excitation of BAAEs since they are shown to have a large damping rate [3], that only reduces for high η_i values [4].

The BAAEs are modes with mixed Alfvén-acoustic polarization. In our model, the polarization of the modes is determined by the S function of Eq.(5). Modes with Alfvénic polarization have $\delta\Phi^{(0)} = \delta\Psi^{(0)}$ and $|S| \sim \beta^{1/2}$ or lower, while modes with significant acoustic component, such as BAAEs are identified by having $|S| \gg \beta^{1/2}$. In the fluid limit of the theory, around the BAE accumulation point $|S| \sim \beta^{1/2}$, which is also the case in the opposite limit $\omega \ll \omega_{bi}$. This

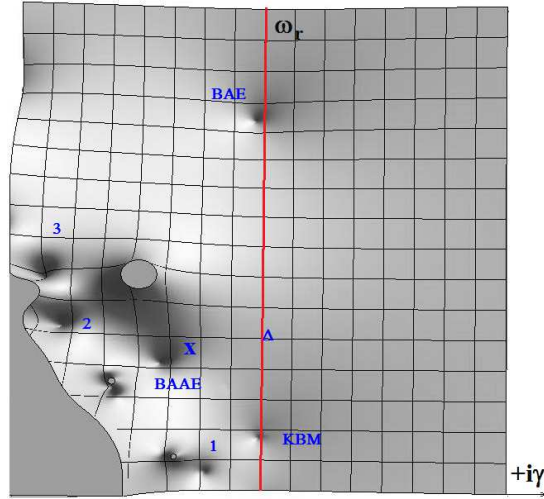


FIG. 1.: Accumulation points of BAE, KBM and BAAE in complex plane for $\eta_i = 0$, $\tau = 1$ and $q = 4/3$. The vertical scale is ω_r , horizontal $i\gamma$, thick red line $\gamma = 0$. 'Δ' marks the BAAE for $\eta_i = 3.5$ and $\Omega_* = 1$, while 'x' marks the KBM for $\eta_i = 1$ and $\Omega_* = 0.8$.

explains the vanishing of the τ term in the Rosenbluth-Hinton Eq.(16). At low η_i the KBM is purely Alfvénic, but for increasing η_i and Ω_* it becomes of mixed polarization, which creates an issue with the identification of the mode as a BAAE or KBM. Detailed discussion of this problem can be found in Ref.[4]. The increase of the diamagnetic frequency can also change the polarization of the BAAE, while decreasing its damping rate. In FIG.1. the BAAE mode for $\eta_i = 3.5$ and $\Omega_* = 1$ is marked with 'Δ'. Here, the BAAE is already unstable, but its frequency is below the EP resonant frequencies and ω_{*pi} . The mode could be driven by a non-resonant EP drive coming from $\delta\bar{W}_f + \delta\bar{W}_k$, as shown by the numerical simulations with GTC code, but this might result with a change of the polarization to Alfvénic [15]. This excitation is non-resonant, i.e. BAAEs would weakly affect EP transport. Additionally, the BAAEs may be excited by the precessional motion of thermal particles through $\delta\bar{W}_k$ in Eq.(18), confirmed by GTC simulations that show power exchange between one of these low frequency modes with the thermal ions at the precession frequency.

When discussing the accumulation points ($\Lambda=0$), the electron temperature only appears through $\tau = T_e/T_i$ in the polarization term, so when S is negligible the mode is not affected by T_e . The KBM frequency $\omega \simeq \omega_{*pi}$ at low η_i is not correlated with the electron temperature. Similarly the accumulation point of the BAAE at $\eta_i = 0$ is not strongly affected by τ , even though the usual assessment is $\omega_{BAAE} \propto (T_e/T_i)^{1/2}$. BAE frequency is strongly dependent of τ since the functions in the denominator of Eq.(5) add up to -1 , which brings forth the $1/\tau$ term. This is not the case for BAAEs, so any significant effects of T_e on this branch is not coming from the accumulation point.

It is important to mention that both the terms $\delta\bar{W}_f$ and I_ϕ also contain τ , so the origin of the effects of T_e and ∇T_e on the modes should be investigated carefully. In the case of the LFM in Ref.[6], increasing T_e drives the mode, but increasing T_i and ∇T_i has stabilizing effects, while the mode frequency is closely following the n mode number. The later is also valid for KBMs at low ω_{*pi} . The effects of electron temperature on these low frequency modes can be fully explained when the RHS of Eq. (1) is taken into account, in which case the mode is localized

slightly off the rational surface. The location of the accumulation point of the mode (rational surface) is determined by the mode numbers and q -profile, while the mode frequency itself by matching the real part of $i\Lambda$ with $Re(\delta\bar{W}_f + \delta\bar{W}_k)$. The imaginary part of $\delta\bar{W}_k$ compensates for the damping on the LHS of GFLDR, i.e. $Im(i\Lambda) = Im(\delta\bar{W}_k)$.

4. CONCLUSIONS

The thermal particles play an important role in the dynamics of the low frequency modes located in the kinetic thermal ion gap, even more than energetic particles themselves. The low frequency Alfvénic mode closely connected with the ion diamagnetic frequency known as KBM, is easier to excite than the mixed polarization BAAE. The latter is however coupled with the KBM through the ion diamagnetic frequency, and becomes marginally unstable only for high Ω_* and η_i , in which case it could be non-resonantly excited by energetic particles. This however can change its polarization to Alfvénic. The precession resonance with thermal ions and electrons, as well as the effects from $\delta\bar{W}_f$ due to energetic particle β and ω_* are worthwhile examining as a drive for some of these modes. Out of the modes mentioned in this work, only the BAEs strongly interact with EPs in tokamak plasma, and can be deleterious to their confinement. The LFMs are known to be driven by high electron temperature, which can be traced to the thermal part of the RHS terms in Eq.(1). The GFLDR is the proper description to explain the linear excitation of the low frequency branches regardless whether they are reactive or resonant, since it contains all the relevant physics of fluctuations in the thermal ion kinetic gap. It is a general and comprehensive tool for understanding mode structures at low frequencies and explaining experimental observations.

ACKNOWLEDGMENT

This work is supported by R&D Program through the Korean Institute of Fusion Energy (KFE) funded by the Ministry of Science and ICT of the Republic of Korea (KFE-EN2141-7).

References

- [1] Gorelenkov, N. N., Berk, et al. Phys. Lett. A **370**, (2007) 70.
- [2] Chen, L., and Zonca, F., Physics of Plasmas **24**, (2017) 072511.
- [3] Zonca, F., Biancalani, A., Chavdarovski, I., Chen, L., Di Troia, C. and Wang, X., Journal of Physics: Conference Series **260** (2010) 012022.
- [4] Chavdarovski, I., and Zonca, F., Plasma Phys **21**, (2014) 052506
- [5] Tsai, S. T., and Chen, L., Phys. Fluids **B 5** (1993) 3284
- [6] Heidbrink, W.W. et al, Nucl. Fusion **61** (2021) 016029 (16pp)
- [7] Zonca, F., Chen, L., and Santoro, R. A. Plasma Phys. Control. Fusion **38** (1996) 2011
- [8] Chavdarovski, I., and Zonca, F., Plasma Phys. Control. Fusion **51**, (2009) 115001 (22pp)
- [9] Chen, L., and Zonca, F., Rev. Mod. Phys. **88**, (2016) 015008
- [10] Rosenbluth, M.N., and Hinton F.L., Phys. Rev. Lett. **80** (1998) 724
- [11] Fulvio, Z., Chen L., Chavdarovski I. et al, "Analytical and numerical gyrokinetic studies of low-frequency drift Alfvén waves in toroidal fusion plasmas" IAEA FEC 2020, IAEA-CN-286/TH/P1-643
- [12] Ma, R., Chavdarovski, I., Ye, G., and Wang, X., Physics of Plasmas **21**, (2014) 062120
- [13] Zonca, F., and Chen, L., Plasma Phys **21**, (2014) 072121
- [14] Chen, L., Phys. Plasmas **1**, (1994) 1519
- [15] Zhang, H.S., Liu, Y.Q., Lin, Z., and Zhang, W.L., Phys. Plasmas **23** (2016) 042510